Nanoscale Research Letters
a SpringerOpen Journal

**NANO EXPRESS**                                                    **Open Access**

# Single-molecule conductance of dipyridines binding to Ag electrodes measured by electrochemical scanning tunneling microscopy break junction

Xiao-Yi Zhou, Ya-Hao Wang, Han-Mei Qi, Ju-Fang Zheng, Zhen-Jiang Niu and Xiao-Shun Zhou[*]

**Abstract**

We have measured the conductance of three pyridyl-terminated molecules binding to Ag electrodes by using electrochemical jump-to-contact scanning tunneling microscopy break junction approach (ECSTM-BJ). Three molecules, including 4,4'-bipyridine (BPY), 1,2-di(pyridin-4-yl)ethene (BPY-EE), and 1,2-di(pyridin-4-yl)ethane (BPY-EA), contacting with Ag electrodes show three sets of conductance values, which follow the order of BPY > BPY-EE > BPY-EA. These values are smaller than those of molecules with Au electrodes, but larger than those of molecules with Cu electrodes. The difference may attribute to the different electronic coupling efficiencies between the molecules and electrodes. Moreover, the influence of the electrochemical potential on the Fermi level of electrodes is also discussed.

**Keywords:** Sliver; Single-molecule junctions; STM-BJ; Charge transport; Electrochemistry

## Background

Single metal-molecule-metal junctions have attracted much attention for their fundamentally important role in molecular electronics [1-3]. While the molecular structure is demonstrated to influence the charge transport through single-molecule conductance [4,5], the contact between electrode and molecule also plays an important role [6,7]. For example, the electrode materials can influence the electronic coupling between electrodes and molecules, such as the interaction of electrode-anchoring group and the alignment of the energy level of electrode-molecule [8,9]. Typically, most of the conductance measurements of single-molecule junctions were performed by using Au as electrode for its chemically inert property [10]. However, it is also important to study the non-Au electrodes to fully understand the charge transport through single-molecule junctions. We pay attention to the Ag electrodes for the following reasons: Ag has strong optical enhancement property and high catalytic activity [10-12]. It has a similar electronic structure with Au and Cu and is easy for comparison among them.
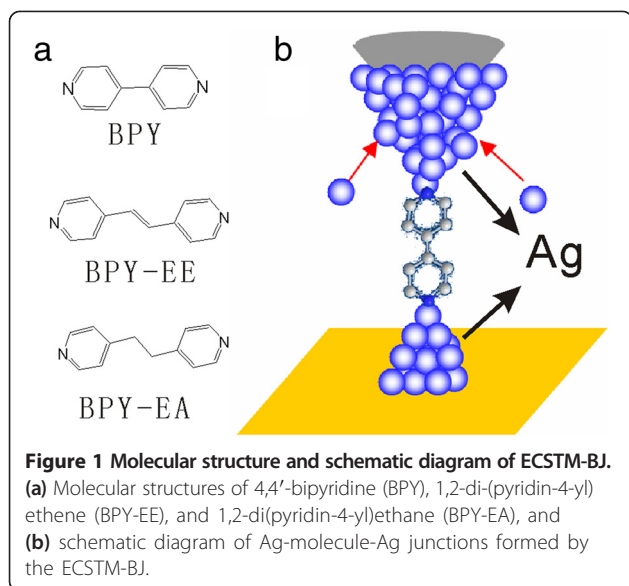
Single-molecule conductance can be measured by scanning tunneling microscopy (STM) break junction (STM-BJ), mechanically controllable break junction (MCBJ), STM trapping and conducting atomic force microscopy, and so on [13-21]. Though lots of works have been done on the electron transport of single-molecule junctions by using the above methods, there is limited investigation on single-molecule junctions with non-Au electrodes [10,22].

We have developed an electrochemical jump-to-contact scanning tunneling microscopy break junction approach (ECSTM-BJ) [23]. By using this approach, single-molecule junctions with carboxylic acid binding to different metallic electrodes were systematically investigated [9,24]. Since the pyridyl group also has received much attention [15,17,25-27], we recently extended this approach to the conductance measurement of pyridyl-based molecules binding to Cu electrode, which shows that the single-molecule conductance with pyridyl-Cu contacts is smaller than that with pyridyl-Au contacts [28]. In this work, we focus on the single-molecule junctions with pyridyl group (Figure 1a) binding to Ag contacts by ECSTM-BJ. Especially, the

* Correspondence: xszhou@zjnu.edu.cn
Zhejiang Key Laboratory for Reactive Chemistry on Solid Surfaces, Institute of Physical Chemistry, Zhejiang Normal University, Jinhua, Zhejiang 321004, China

Springer

**Figure 1 Molecular structure and schematic diagram of ECSTM-BJ.**
**(a)** Molecular structures of 4,4′-bipyridine (BPY), 1,2-di-(pyridin-4-yl)
ethene (BPY-EE), and 1,2-di(pyridin-4-yl)ethane (BPY-EA), and
**(b)** schematic diagram of Ag-molecule-Ag junctions formed by
the ECSTM-BJ.

influence of the electrochemical potential on the Fermi
level of electrode is discussed.

## Methods

Au(111) was used as substrate, and mechanically cut Pt-Ir
($\Phi$ = 0.25 mm) wires were used as the tips. The latter was
insulated by the thermosetting polyethylene glue to reduce
the leakage current of the electrochemical reaction. Ag
and Pt wire were used as the reference and counter elec-
trodes, respectively. 1,2-Di(pyridin-4-yl)ethene (BPY-EE)
and 1,2-di(pyridin-4-yl)ethane (BPY-EA) were purchased
from Sigma-Aldrich Corp. (St. Louis, MO, USA), while
4,4′-bipyridine (BPY) and $Ag_2SO_4$ (99.999%) were pur-
chased from Alfa Aesar (Ward Hill, MA, USA). $H_2SO_4$
was purchased from Sinopharm Chemical Reagent Co.,
Ltd. (Shanghai, China). All aqueous solutions were pre-
pared with ultrapure water (>18 MΩ cm).

The conductance of the Ag-molecule-Ag junctions
was measured by repeatedly forming and breaking the
molecular junctions on the modified Nanoscope IIIa
STM (Veeco Instruments, Inc., Plainview, NY, USA),
and the process was described in detail in our previously
reports (Figure 1b) [9,28]. To achieve this process, Ag
was continuously electrodeposited onto the STM tip.
Then, the deposited tip was pulled far away from the
substrate about several tens of nanometers with the
STM feedback disabled. Next, the tip was driven towards
the surface until a certain tip current was reached; the
atoms of the deposited metal on the tip would transfer
to the substrate upon the application of a pulse on the
*z*-piezo of STM, and this is the so-called jump-to-
contact process. Atomic-sized wire of the deposited
metal could be obtained by pulling the tip out of the

contact. Lastly, the molecular junctions with the deposited
metal as electrode were formed after breaking of the
atomic-sized metal wire. Conductance curves were re-
corded at the same time. Then, we moved the tip to other
positions and repeated the whole process. Typically, large
conductance traces were obtained, and hundreds from
thousands traces with clear stepwise features were selected
to get a statistical result. The selection rate is around 15%,
which is similar as that of pyridyl-Cu contact in an acidic
solution in our previously report [28]. The low selection
rate may be caused by the protonated pyridyl group [28].
All experiments were carried out at a fixed bias voltage of
50 mV.

## Results and discussion

### Conductance of BPY-EE contacting with Ag electrodes

The conductance of Ag-(BPY-EE)-Ag junctions was
measured in 0.05 M $H_2SO_4$ aqueous solution containing
1 mM $Ag_2SO_4$ and 0.5 mM BPY-EE by using the
ECSTM-BJ approach. In order to avoid the deposition of
$Ag^+$ and pyridyl group in a neutral solution, the acidic
supporting electrolyte was used. Though the pyridyl
group is in protonated form in this acidic solution, it
may contact with the electrode through a deprotonated
form [28]. The Au(111) substrate and Pt-Ir tip were set
at 45 and −5 mV vs the Ag wire, respectively.

Figure 2a shows the typical conductance curves of
Ag-(BPY-EE)-Ag, presenting a rapid drop from step of
$58 \pm 32$ nS (($7.5 \pm 4.2) \times 10^{-4}$ $G_0$). The one-dimensional
conductance histogram constructed from hundreds of
such individual conductance traces reveals single-molecule
conductance values of $58 \pm 32$ nS (Figure 2b), and the con-
ductance value is the same as that of a two-dimensional
(2D) histogram (Figure 2c), which is constructed by count-
ing the number of data at each conductance value with
each stretching distance from the conductance curves
[9,29]. In other words, individual data points are binned in
a two-dimensional histogram (the bin size for the distance
is 0.005 nm), while the conductance value for the (BPY-
EE)-Ag contact in Figure 2c is 8.9 nS (0.89 nS for Figure 3c
and 0.056 nS for Figure 3f). Typically, a conductance value
close to a saturated range of the scanner amplifier was set
for zero distance in the 2D histograms. The high counts
can represent the most typical breaking behavior of the
molecular junctions in such 2D histogram. We can also
get the $10 \times 10$ arrays of the Ag clusters, which were
formed simultaneously by the breaking of the junctions
as shown in Figure 2d.

Two more sets of conductance values $7.0 \pm 3.5$ nS
(($0.90 \pm 0.46) \times 10^{-4}$ $G_0$) (Figure 3a,b,c) and $1.7 \pm 1.1$ nS
(($0.22 \pm 0.14) \times 10^{-4}$ $G_0$) (Figure 3d,e,f) were also found
for the Ag-(BPY-EE)-Ag junctions. These are consistent
with the contacts with Cu and Au, which also have three
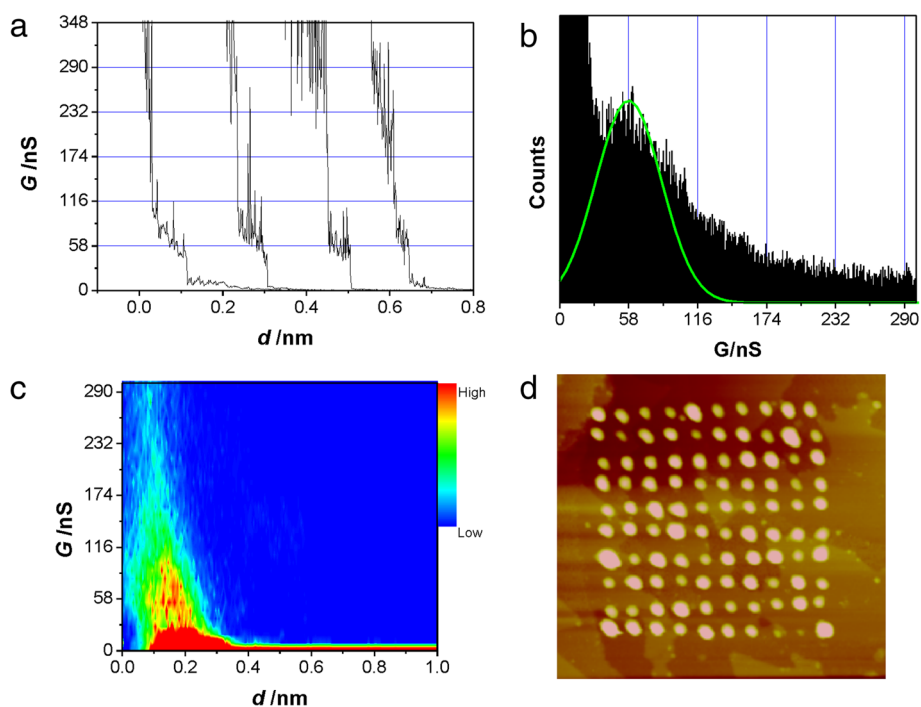sets of conductance values [17,27,28]. The multiple

**Figure 2 High conductance of the Ag-(BPY-EE)-Ag junctions. (a)** Typical conductance curves for high conductance (HC) of Ag-(BPY-EE)-Ag junctions. **(b)** 1D and **(c)** 2D conductance histogram of the Ag-(BPY-EE)-Ag junctions constructed from the curves shown in **(a)**. **(d)** The STM image (150 × 150 nm$^2$) of a 10 × 10 array of Ag clusters simultaneously generated with the conductance curves.

conductance values can be contributed to the different contact configurations between the electrode and anchoring group [7,30]. The conductance values 58 ± 32, 7.0 ± 3.5, and 1.7 ± 1.1 nS can be denoted as high conductance (HC), medium conductance (MC), and low conductance (LC), respectively. Taking the HC value as example, the conductance values for pyridyl-Cu and pyridyl-Au are 45 and 165 nS, respectively, as reported by our group [28]. The conductance value of pyridyl-Ag is in between them. Moreover, it also shows the same order for the MC and LC with different metal electrodes. The different conductance values can be contributed to the different electronic coupling efficiencies between the molecules and electrodes [9]. We will discuss it later.

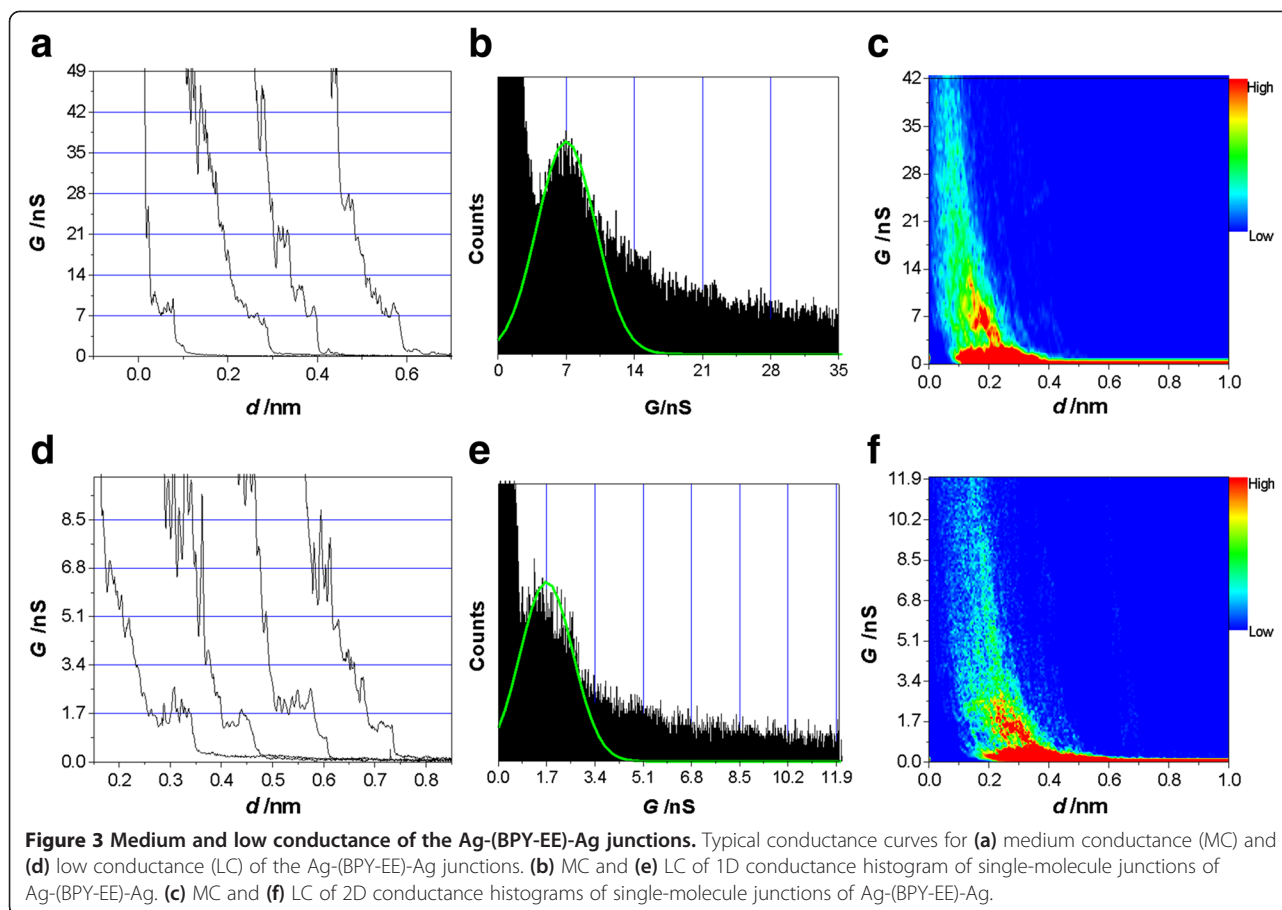## Conductance of BPY and BPY-EA contacting with Ag electrodes

We also carried out the conductance measurement of BPY and BPY-EA contacting with Ag electrodes by using the same method. The results are shown in Figure 4. The HC, MC, and LC of BPY are 140 ± 83 nS ((18.1 ± 10.7) × $10^{-4}$ $G_0$), 19.0 ± 8.8 nS ((2.4 ± 1.1) × $10^{-4}$ $G_0$), and 6.0 ± 3.8 nS ((0.78 ± 0.49) × $10^{-4}$ $G_0$), while those of BPY-EA are 14.0 ± 8.8 nS ((1.8 ± 1.1) × $10^{-4}$ $G_0$), 2.4 ± 1.1 nS ((0.31 ±

0.14) × $10^{-4}$ $G_0$), and 0.38 ± 0.16 nS ((0.049 ± 0.021) × $10^{-4}$ $G_0$), respectively. The single-molecule conductance values of BPY, BPY-EE, and BPY-EA are summarized in Table 1.

Taking the HCs of BPY (140 ± 83 nS), BPY-EE (58 ± 32 nS), and BPY-EA (14.0 ± 8.8 nS) as examples, the conductance of BPY is about twice that of BPY-EE, and 10 times that of BPY-EA. Though BPY-EE and BPY-EA have similar lengths of 0.95 nm, BPY-EE is kept with conjugated backbone, while the conjugated backbone is interrupted by the insertion of $CH_2CH_2$ in BPY-EA [25,31]. These facts have contributed to the big difference between the conductance of BPY-EE and BPY-EA. The conductance values of BPY and BPY-EA contacting with Ag are also in between those of BPY and BPY-EA contacting with Au and Cu electrodes.

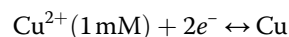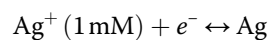## The influence of the metal electrodes on the single-molecule conductance

Now, we will focus on the influence of metal electrodes on the single-molecule conductance. We compare the single-molecule conductance contacting with Ag, Au, and Cu electrodes. Taking the HC as example, the conductance value of pyridyl-Ag is between the values of pyridyl-Au and pyridyl-Cu as shown in Figure 5. It is in

**Figure 3 Medium and low conductance of the Ag-(BPY-EE)-Ag junctions.** Typical conductance curves for **(a)** medium conductance (MC) and **(d)** low conductance (LC) of the Ag-(BPY-EE)-Ag junctions. **(b)** MC and **(e)** LC of 1D conductance histogram of single-molecule junctions of Ag-(BPY-EE)-Ag. **(c)** MC and **(f)** LC of 2D conductance histograms of single-molecule junctions of Ag-(BPY-EE)-Ag.
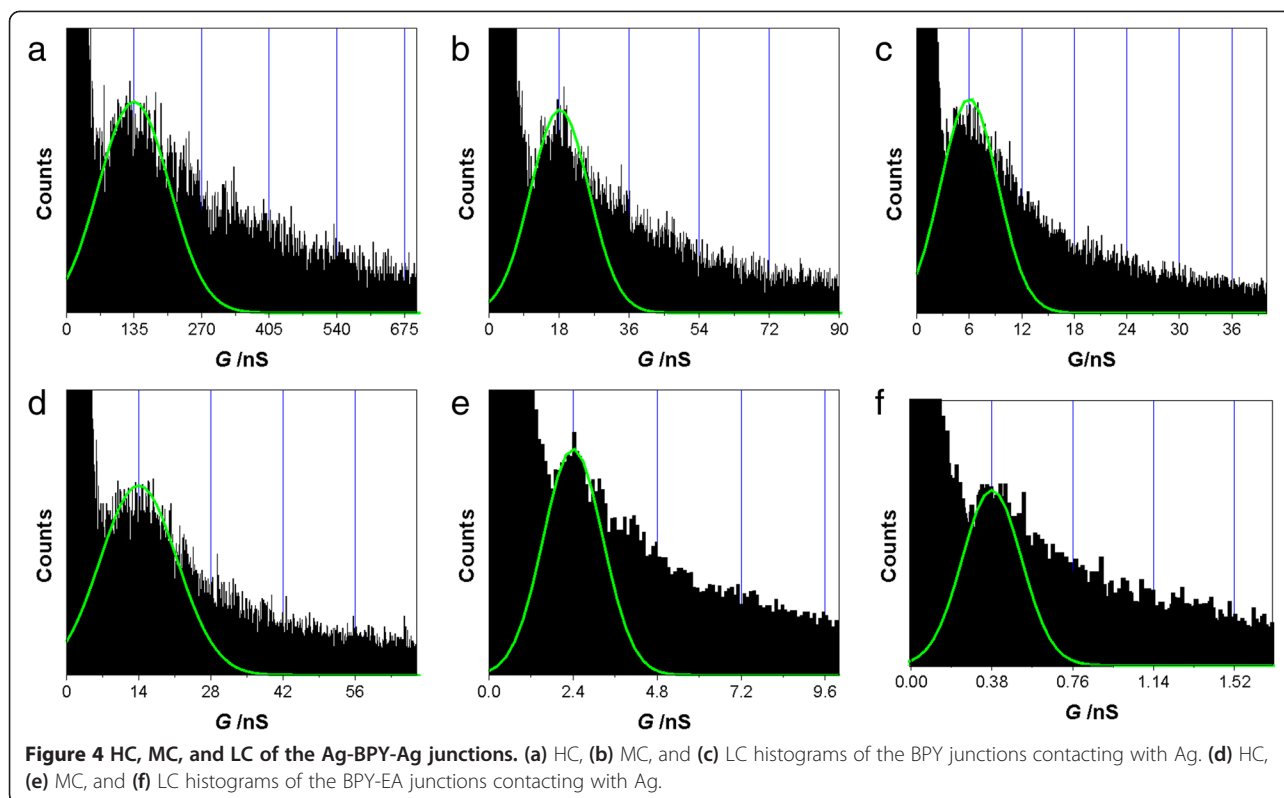
the same order for the MC and LC with different metal electrodes. It was reported that the binding interaction of pyridyl with Ag, Cu, and Au follows the order of pyridyl-Cu ~ pyridyl-Au > pyridyl-Ag by theoretical calculation [32], which is different from the conductance value order of pyridyl-Au > pyridyl-Ag > pyridyl-Cu. Thus, the conductance difference may mainly be contributed to the efficiency of electron transport along the molecule for Cu, Au, and Ag [28].

It was reported that the LUMO is the essential orbital channel for the electron transport in the Au-BPY-Au junction without potential control of the electrodes [26,27]. However, the situation may be complex in the current experiment with the control of the electrode potential. The Fermi level of the electrode would be changed by the potential. Usually, the Fermi energy of the hydrogen reference electrode under standard conditions (SHE) is considered as the zero energy in electrochemistry, while the energy of SHE is very close to 4.44 eV [33]. Typically, the standard potentials for the $Ag^+|Ag$ and $Cu^{2+}|Cu$ are 0.80 V (SHE) and 0.34 V (SHE), respectively [34]. If we consider the influence of the concentrations of the

metal ion (1 mM $Ag_2SO_4$ and 1 mM $CuSO_4$), the potentials for the equilibria

$$Ag^+(1\,mM) + e^- \leftrightarrow Ag$$

$$Cu^{2+}(1\,mM) + 2e^- \leftrightarrow Cu$$

are 0.64 V (SHE) and 0.25 V (SHE), respectively. We also measured the potentials of the $Ag^+|Ag$ in the aqueous solution containing 0.05 M $H_2SO_4$ + 1 mM $Ag_2SO_4$ + 0.5 mM BPY and $Cu^{2+}|Cu$ in the 0.05 M $H_2SO_4$ + 1 mM $CuSO_4$ + 0.5 mM BPY, which give out the 0.65 V (SHE) for $Ag^+|Ag$ and 0.25 V (SHE) for $Cu^{2+}|Cu$. Correspondingly, these values are similar with the above calculated values. We can infer that the Fermi energy levels for $Ag^+|Ag$ and $Cu^{2+}|Cu$ are −5.09 and −4.69 eV from the measured potentials, respectively. For the Au electrode, we found that the potential of Au wire is about 0.45 V in 50 mM $H_2SO_4$ + 0.5 mM BPY and give out −4.89 eV for the Fermi energy of Au. Returning back to our experiments, the electrodes were controlled near the potentials of the reference wires (Ag, Cu, and Au) [28]; thus the Fermi energy of the electrode may also be approximated to these energy levels. However, these values

**Figure 4 HC, MC, and LC of the Ag-BPY-Ag junctions. (a)** HC, **(b)** MC, and **(c)** LC histograms of the BPY junctions contacting with Ag. **(d)** HC, **(e)** MC, and **(f)** LC histograms of the BPY-EA junctions contacting with Ag.

are quite different from the Fermi energy of Au (−5.13 eV), Ag (−4.65 eV), and Cu (−4.26 eV) in vacuum [35], and may change the essential orbital channel of the molecules.

It is not possible to know which orbital channel (such as HOMO or LUMO) is actually the most favorable in the current study. However, the conductance order of the single-molecule junctions with different metallic electrodes is caused by the different coupling efficiency between the metallic electrodes and the anchoring group, and also the molecular energy levels and Fermi energy level of the electrodes [8,9]. Further calculations are needed to fully understand the influence of the metallic electrodes.
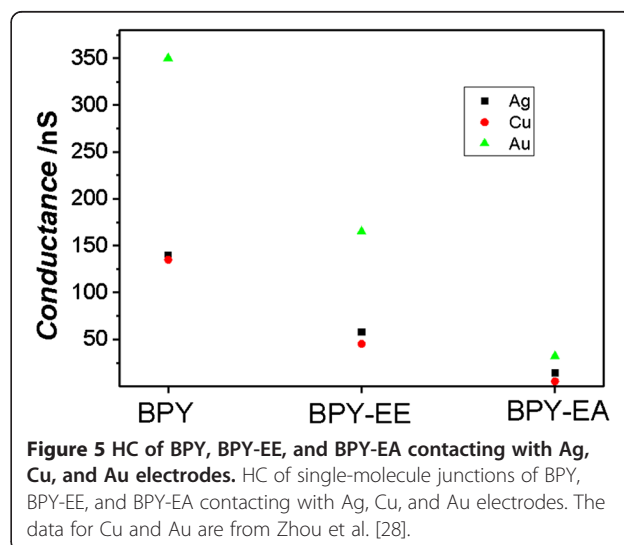
## Conclusions

We have measured the single-molecule conductance of pyridine-terminated molecules contacting with Ag electrodes. All three molecules (BPY, BPY-EE, and BPY-EA) have three sets of conductance values and show the order of BPY > BPY-EE > BPY-EA. These values are larger than those of molecules with the Cu electrodes, but smaller than those of molecules with the Au electrodes. The different single-molecule conductance between Ag, Cu, and Au electrodes can be attributed to the different electronic coupling efficiencies between the molecules and electrodes.



**Figure 5 HC of BPY, BPY-EE, and BPY-EA contacting with Ag, Cu, and Au electrodes.** HC of single-molecule junctions of BPY, BPY-EE, and BPY-EA contacting with Ag, Cu, and Au electrodes. The data for Cu and Au are from Zhou et al. [28].

**Table 1 Summary of single-molecule conductance with contact of the Ag electrodes**

| Molecules | HC (nS) | MC (nS) | LC (nS) |
|---|---|---|---|
| BPY | 140 ± 83 | 19.0 ± 8.8 | 6.0 ± 3.8 |
| BPY-EE | 58 ± 32 | 7.0 ± 3.5 | 1.7 ± 1.1 |
| BPY-EA | 14.0 ± 8.8 | 2.4 ± 1.1 | 0.38 ± 0.16 |

## Authors' information

XYZ is a Master's degree student under the supervision of XSZ in the Institute of Physical Chemistry, Zhejiang Normal University, China.

## References

1. Bruot C, Hihath J, Tao NJ: **Mechanically controlled molecular orbital alignment in single molecule junctions.** *Nat Nanotechnol* 2012, **7**:35–40.
2. Kiguchi M, Kaneko S: **Single molecule bridging between metal electrodes.** *Phys Chem Chem Phys* 2013, **15**:2253–2267.
3. Song H, Reed MA, Lee T: **Single molecule electronic devices.** *Adv Mater* 2011, **23**:1583–1608.
4. Venkataraman L, Klare JE, Nuckolls C, Hybertsen MS, Steigerwald ML: **Dependence of single-molecule junction conductance on molecular conformation.** *Nature* 2006, **442**:904–907.
5. He J, Chen F, Li J, Sankey OF, Terazono Y, Herrero C, Gust D, Moore TA, Moore AL, Lindsay SM: **Electronic decay constant of carotenoid polyenes from single-molecule measurements.** *J Am Chem Soc* 2005, **127**:1384–1385.
6. Chen F, Li XL, Hihath J, Huang ZF, Tao NJ: **Effect of anchoring groups on single-molecule conductance: comparative study of thiol-, amine-, and carboxylic-acid-terminated molecules.** *J Am Chem Soc* 2006, **128**:15874–15881.
7. Li XL, He J, Hihath J, Xu BQ, Lindsay SM, Tao NJ: **Conductance of single alkanedithiols: conduction mechanism and effect of molecule-electrode contacts.** *J Am Chem Soc* 2006, **128**:2135–2141.
8. Ko CH, Huang MJ, Fu MD, Chen CH: **Superior contact for single-molecule conductance: electronic coupling of thiolate and isothiocyanate on Pt, Pd, and Au.** *J Am Chem Soc* 2010, **132**:756–764.
9. Peng ZL, Chen ZB, Zhou XY, Sun YY, Liang JH, Niu ZJ, Zhou XS, Mao BW: **Single molecule conductance of carboxylic acids contacting Ag and Cu electrodes.** *J Phys Chem C* 2012, **116**:21699–21705.
10. Kim T, Vázquez H, Hybertsen MS, Venkataraman L: **Conductance of molecular junctions formed with silver electrodes.** *Nano Lett* 2013, **13**:3358–3364.
11. Cui L, Chen P, Chen S, Yuan Z, Yu C, Ren B, Zhang K: **In situ study of the antibacterial activity and mechanism of action of silver nanoparticles by surface-enhanced Raman spectroscopy.** *Anal Chem* 2013, **85**:5436–5443.
12. van Schrojenstein Lantman EM, Deckert-Gaudig T, Mank AJG, Deckert V, Weckhuysen BM: **Catalytic processes monitored at the nanoscale with tip-enhanced Raman spectroscopy.** *Nat Nano* 2012, **7**:583–586.
13. Ho Choi S, Kim B, Frisbie CD: **Electrical resistance of long conjugated molecular wires.** *Science* 2008, **320**:1482–1486.
14. Sedghi G, Garcia-Suarez VM, Esdaile LJ, Anderson HL, Lambert CJ, Martin S, Bethell D, Higgins SJ, Elliott M, Bennett N, Macdonald JE, Nichols RJ: **Long-range electron tunnelling in oligo-porphyrin molecular wires.** *Nat Nanotechnol* 2011, **6**:517–523.
15. Xu BQ, Tao NJ: **Measurement of single-molecule resistance by repeated formation of molecular junctions.** *Science* 2003, **301**:1221–1223.
16. Chen IWP, Fu M-D, Tseng W-H, Chen C-H, Chou C-M, Luh T-Y: **The effect of molecular conformation on single molecule conductance: measurements of pi-conjugated oligoaryls by STM break junction.** *Chem Commun* 2007, **29**:3074–3076. doi:10.1039/B705521H.
17. Hong W, Manrique DZ, Moreno-García P, Gulcur M, Mishchenko A, Lambert CJ, Bryce MR, Wandlowski T: **Single molecular conductance of tolanes: experimental and theoretical study on the junction evolution dependent on the anchoring group.** *J Am Chem Soc* 2012, **134**:2292–2304.
18. Tian JH, Yang Y, Liu B, Schollhorn B, Wu DY, Maisonhaute E, Muns AS, Chen Y, Amatore C, Tao NJ, Tian ZQ: **The fabrication and characterization of adjustable nanogaps between gold electrodes on chip for electrical measurement of single molecules.** *Nanotechnology* 2010, **21**:274012.
19. Haiss W, van Zalinge H, Higgins SJ, Bethell D, Hobenreich H, Schiffrin DJ, Nichols RJ: **Redox state dependence of single molecule conductivity.** *J Am Chem Soc* 2003, **125**:15294–15295.
20. Diez-Perez I, Hihath J, Hines T, Wang Z-S, Zhou G, Mullen K, Tao N: **Controlling single-molecule conductance through lateral coupling of pi orbitals.** *Nat Nanotechnol* 2011, **6**:226–231.
21. Arroyo CR, Frisenda R, Moth-Poulsen K, Seldenthuis JS, Bjornholm T, van der Zant HSJ: **Quantum interference effects at room temperature in OPV-based single-molecule junctions.** *Nanoscale Res Lett* 2013, **8**:1–6.
22. Kiguchi M, Murakoshi K: **Conductance of single $C_{60}$ molecule bridging metal electrodes.** *J Phys Chem C* 2008, **112**:8140–8143.
23. Zhou XS, Wei YM, Liu L, Chen ZB, Tang J, Mao BW: **Extending the capability of STM break junction for conductance measurement of atomic-size nanowires: an electrochemical strategy.** *J Am Chem Soc* 2008, **130**:13228–13230.
24. Zhou XS, Liang JH, Chen ZB, Mao BW: **An electrochemical jump-to-contact STM-break junction approach to construct single molecular junctions with different metallic electrodes.** *Electrochem Commun* 2011, **13**:407–410.
25. Zhou XS, Chen ZB, Liu SH, Jin S, Liu L, Zhang HM, Xie ZX, Jiang YB, Mao BW: **Single molecule conductance of dipyridines with conjugated ethene and nonconjugated ethane bridging group.** *J Phys Chem C* 2008, **112**:3935–3940.
26. Quek SY, Kamenetska M, Steigerwald ML, Choi HJ, Louie SG, Hybertsen MS, Neaton JB, Venkataraman L: **Mechanically controlled binary conductance switching of a single-molecule junction.** *Nat Nanotechnol* 2009, **4**:230–234.
27. Wang C, Batsanov AS, Bryce MR, Martin S, Nichols RJ, Higgins SJ, Garcia-Suarez VM, Lambert CJ: **Oligoyne single molecule wires.** *J Am Chem Soc* 2009, **131**:15647–15654.
28. Zhou XY, Peng ZL, Sun YY, Wang LN, Niu ZJ, Zhou XS: **Conductance measurement of pyridyl-based single molecule junctions with Cu and Au contacts.** *Nanotechnology* 2013, **24**:465204.
29. Martin CA, Ding D, Sorensen JK, Bjornholm T, van Ruitenbeek JM, van der Zant HSJ: **Fullerene-based anchoring groups for molecular electronics.** *J Am Chem Soc* 2008, **130**:13198–13199.
30. Li C, Pobelov I, Wandlowski T, Bagrets A, Arnold A, Evers F: **Charge transport in single Au|alkanedithiol|Au junctions: coordination geometries and conformational degrees of freedom.** *J Am Chem Soc* 2008, **130**:318–326.
31. Kamenetska M, Quek SY, Whalley AC, Steigerwald ML, Choi HJ, Louie SG, Nuckolls C, Hybertsen MS, Neaton JB, Venkataraman L: **Conductance and geometry of pyridine-linked single-molecule junctions.** *J Am Chem Soc* 2010, **132**:6817–6821.
32. Wu DY, Li JF, Ren B, Tian ZQ: **Electrochemical surface-enhanced Raman spectroscopy of nanostructures.** *Chem Soc Rev* 2008, **37**:1025–1041.
33. Morrison RS: *Electrochemistry at Semiconductor and Oxidized Metal Electrodes.* New York: Plenum; 1980.
34. Bratsch SG: **Standard electrode potentials and temperature coefficients in water at 298.15 K.** *J Phys Chem Ref Data* 1989, **18**:1–21.
35. Michaelson HB: **The work function of the elements and its periodicity.** *J Appl Phys* 1977, **48**:4729–4733.